Photo-Induced Copper-Mediated Acrylate Polymerization in Continuous-Flow Reactors

Svitlana Railian[1], Benjamin Wenn[1] and Thomas Junkers[1,2]*

[1]*Polymer Reaction Design Group, Institute for Materials Research (IMO), Universiteit Hasselt, Martelarenlaan 42, B-3500 Hasselt, Belgium*
[2]*IMEC Associated Lab IMOMEC, Wetenschapspark 1, B-3590 Diepenbeek, Belgium*

Received: 29 April 2016; accepted: 21 June 2016

The synthetic scope of photo-induced copper-mediated polymerization (photoCMP) in continuous-flow reactors is further explored. A series of monomers, namely, methyl (MA), ethyl (EA), *n*-butyl (*n*BA), 2-hydroxyethyl (HEA), and di(ethylene glycol) ethyl ether (DEGA) acrylate are investigated, all showing high livingness (dispersity in the range of 1.1 and linear first order kinetics) in the polymerizations and high conversions within 20-min reaction time. Next to the commonly used solvent (dimethyl sulfoxide [DMSO]), also a water–ethanol mixture was used as greener alternative, without any loss in reaction control. Upscaling the reactor from 2 to 16 mL allows for production of over 200 g of high-definition material (3000 g/mol, 1.1 dispersity) in overnight operation (18 h), demonstrating that the photoprocess can be run under very stable conditions even for extended reaction times. Via coupling of two reactors, direct chain extension of copolymers in a single reaction step is also demonstrated.

Keywords: photopolymerization, controlled polymerization, block copolymers, upscaling, flow chemistry

1. Introduction

Photochemistry is an old branch of chemistry but, to date, has only played a minor role in materials synthesis outside of curing processes and some highly specific applications in natural product synthesis, despite the enormous potential of photoreactions with regards to reaction efficiencies and, in principle, advantageous economy and ecology of light-induced reactions. With the increasing popularity of continuous-flow reactors, photochemistry regained focus of academic as well as industrial research [1]. Usage of photochemically triggered reactions allows for reaction pathways and mechanisms which are not or only indirectly accessible with thermally induced reactions. Yet, the main drawback of light-induced reactions so far was always issues occurring with respect to scalability. Due to Beer–Lambert's law, light gradients develop in any photoreaction carried out in batch due to successive light absorption with increasing optical pathlength, penalizing the efficiency of the reaction in that the desired chemical transformations mostly only take place at the reactor wall whereas the bulk of the reaction mixture remains a dead volume [2]. This problem might be negligible on small scale lab experiments but becomes rapidly significant in reaction upscaling, already at an intermediate laboratory scale. Continuous-flow reactors, however, can give an essential advantage and be a game changer for application of photochemistry in (scalable) synthesis. In continuous-flow reactors, reactions are mostly performed in thin reaction channels which guarantee normally good heat transfer but, at the same time, also allow for avoidance of light intensity gradients [2]. Continuous-flow reactors in laboratories are often made out of fluoropolymer tubing with a diameter of less than 2 mm [3]. With average extinction coefficients, these diameters are small enough to not cause significant radial light gradients, and hence, the problems with upscaling of photoreactions are entirely avoided [2]. Despite the small diameters, larger reactor volumes are still easily achieved by increasing the tubing length or via reactor parallelization [4].

Within the realm of polymer chemistry, the large potential of using (photo) flow reactors for the synthesis of precision polymer materials has only recently emerged [2]. Precision polymer materials are commonly synthesized via living polymerization techniques, more specifically via reversible deactivation radical polymerization (RDRP) methods. RDRP gives access to polymers with high definition, narrow dispersity, and sophisticated control over the macromolecular architecture, and already for thermal RDRP, the advantage of using flow reactions has been demonstrated [5]. The most applied RDRP methods are the so-called reversible addition–fragmentation chain transfer polymerization (RAFT) [6], nitroxide mediated polymerization (NMP) [7], and transition metal-mediated polymerization [8] such as atom transfer radical polymerization (ATRP) [9] and single-electron transfer living radical polymerization (SET-LRP) [10]. In the past years, for all main RDRP methods, photo-induced processes have also been discovered and investigated [11]. Successful photo-induced transition metal-mediated polymerizations are reported in literature, and a broad range of catalysts has been used, with cobalt [12], iron [13], iridium [14], and copper [15] being the most important examples. Junkers and coworkers described first the combination of photo-induced copper-mediated polymerization (photoCMP) and continuous-flow reactors, based on the batch concept introduced by the Haddleton group [15a]. First, only the polymerization of acrylates [16]. was studied, followed by the synthesis of poly(methacrylates) and methacrylate–acrylate block copolymers in flow [17]. Next to such linear block copolymer structures, recently, also the (flow) synthesis of star-shaped multiblock copolymers via photoCMP was investigated [18]. As mentioned above, photoflow polymerizations are also reported for cobalt [19] and iridium-mediated [20] reactions. PhotoCMP was also successfully applied for grafting on silicon surfaces [21] or to make sequence-defined oligomers with biological precision, albeit not in continuous flow [22]. Additionally, two groups reported lately on successful photo-induced RAFT polymerization in flow reactors [23]. Baeten et al. used a photoflow microreactor for inline ultraviolet (UV) modification of phosphoesters via a thiol-ene reaction [24].

While photoRDRP [25] has very interesting features such as enhanced structural fidelity and ability for spatiotemporal control, its potential as a pure synthetic tool (where spatial control plays no major role) is, to date, vastly unexplored, also owing to the scalability gap outlined above. In here, we extend our initial proof of principle work on photoCMP in continuous-flow

* Author for correspondence: thomas.junkers@uhasselt.be

DOI: 10.1556/1846.2016.00018

First published online: 15 August 2016

reactors [16] and demonstrate the high versatility of the technique. Continuous-flow synthesis is demonstrated for a range of (acrylic) monomers, under variation of chain length. Also, the reaction solvent is varied in order to reach greener reaction conditions (note that classical photoCMP required DMSO as solvent, which is certainly not sustainable with respect to commercial application). The first upscale for continuous photoflow polymerization on lab scale is presented. In the final step, a two-stage flow reactor for direct chain extension without intermediate isolation step is described. Each of these developments marks a significant advancement for the applicability of photoCMP to flow reactors, and together, the data presented herein may serve as a starting point for even more diversified synthesis of polymers following the photoCMP concept.

2. Experimental

2.1. Materials. Ethyl 2-bromoisbutyrate (EBiB, Alfa Aesar, 98+%), copper (II) bromide ($CuBr_2$, Sigma-Aldrich, 99%), ethanol (EtOH Merck, pro analysis), and dimethyl sulfoxide (DMSO, Merck, pro analysis) were all used as received. Tris-(2-(dimethylamino)ethyl)amine (Me_6TREN) [26] and 2-hydroxyethyl 2′-methyl-2′bromopropionate (HMB) [27] were synthesized following literature procedures. Methyl acrylate (MA, Acros, 99%), ethyl acrylate (EA, Acros, 99.5%), di(ethylene glycol) ethyl ether acrylate (DEGA, TCI, 98%), 2-hydroxyethyl acrylate (HEA, TCI, 95%), and *n*-butyl acrylate (*n*BA, Acros, 99%) were deinhibited over a column of activated basic alumina, prior to use. Additionally, 2-hydroxyethyl acrylate (HEA, TCI, 95%) was purified by distillation.

2.2. Methods. ^{1}H NMR spectra were recorded in deuterated chloroform applying a pulse delay of 12 s with Oxford Instruments Ltd. NMR spectrometers (300 and 400 MHz).

Analytical size exclusion chromatography (SEC) was performed on a Tosoh EcoSEC HLC-8320GPC, comprising an autosampler, a PSS guard column SDV (50 × 7.5 mm), followed by three PSS SDV analytical linear XL (5 μm, 300 × 7.5 mm) columns thermostatted at 40 °C (column molecular weight range: 1×10^2 to 1×10^6 g/mol), and a differential refractive index detector (Tosoh EcoSEC RI) using THF as the eluent with a flow rate of 1 mL/min. Toluene was used as a flow marker. Calibration was performed using linear narrow polystyrene (PS) standards from PSS Laboratories in the range of 470–7.5×10^6 g/mol. For the analysis, the following MHKS parameters were used: for MA, EA, and HEA, $\alpha = 0.74$, $K = 10.2 \times 10^{-5}$ dL/g in THF at 30 °C [28]; for *n*BA, $\alpha = 0.70$, $K = 12.2 \times 10^{-5}$ dL/g in THF at 40 °C [29]; and for DEGA, $\alpha = 0.714$, $K = 13.63 \times 10^{-5}$ dL/g, THF 30 °C at 633 nm for PS [30].

The continuous photoflow reactors were built up out of a 4.5-m perfluoroalkoxy (PFA) tubing (Advanced Polymer Tubing GmbH; outer diameter, 1/16″; inner diameter, 0.75 mm; reactor volume, 2 mL) wrapped around a Vilbour Lourmant 15 W UV-light tube ($\lambda_{max} = 365$ nm). A syringe pump (Chemyx Fusion 100) was used to inject the reaction solutions into the reactor. The lamp heated the reactions to a temperature between 50 and 55 °C. For the scale-up, 20.5 m of PFA tubing with an internal diameter of 1 mm (reactor volume 16 mL) was wrapped around the same lamp. Two Knauer Azura HPLC pumps were used to deliver the reaction solutions. In both reactors, a static T-mixer (Upchurch Scientific, PEEK, swept volume: 0.95 μL, thru-hole: 0.50 mm) was employed. All connections used were purchased from Upchurch Scientific and were made out of PEEK.

Coupled photoflow reactors for the coupled reactors 2.3 m and 3.5 m PFA tubing (Advanced Polymer Tubing GmbH; outer diameter, 1/16″; inner diameter, 0.75 mm; reactor volume, 1 mL and 1.5 mL, respectively) were wrapped around a 15 W UV-light tube (Vilbour Lourmant, $\lambda_{max} = 365$ nm). The reaction solutions were loaded into two Norm-Ject plastic syringes, and a Chemyx Fusion 100 syringe pump was used to deliver the solutions. For fast reaction solution mixing, a static mixer (Upchurch Scientific, PEEK, swept volume: 0.95 μL, thru-hole: 0.50 mm) was added in the lines before entering the reactor. The exit of the first reactor was coupled to a second static mixer. In this mixer, second monomer solution was also supplied via a Norm-Ject syringe and a Chemyx pump. The lamp created a reaction temperature between 50 and 55 °C. All connections used were purchased from Upchurch Scientific and were made out of PEEK.

2.3. General Polymerization Procedure Using the Continuous Photoflow Reactor. EBiB (1 eq.), $CuBr_2$ (0.02 eq.), and Me_6TREN (0.12 eq.) were mixed in a 20-mL amber volumetric flask which was filled up with DMSO. Twenty milliliters of monomer (25–500 eq.) were filled into a separate amber volumetric flask, and both were purged with nitrogen gas for approximately 15 min. The solutions were transferred into Norm-Ject plastic syringes and placed in the syringe pump. Different reaction times were screened via adjusting the flow rate (between 0.025 and 1 mL/min).

2.4. Polymerization of DEGA in a Water–Ethanol Mixture. Before purging for 15 min with nitrogen gas, one amber volumetric flask was filled with DEGA (25–100 eq.) and another one with HMB (1 eq.), $CuBr_2$ (0.02 eq.), Me_6TREN (0.12 eq.), and a 50:50 vol% H_2O–EtOH mixture. The oxygen free solutions were loaded into two Norm-Ject syringes, and a syringe pump was used to deliver the solutions into the reactor. By changing the flow rates, several reaction times were screened.

2.5. One-Step Chain Extension of DEGA in a Water–Ethanol Mixture. In a 10-mL amber volumetric flask, 0.42 g (2.16 mmol, 1 eq.) HMB, 0.01 g (0.04 mmol, 0.02 eq.) $CuBr_2$, and 0.06 g (0.26 mmol, 0.12 eq.) Me_6TREN were dissolved in a 50:50 vol% H_2O–EtOH mixture. This solution and 10 mL DEGA were purged for 10 min with nitrogen and transferred into two syringes. For second monomer addition, 5 mL DEGA was mixed with 5 mL 50:50 vol% H_2O–EtOH mixture, purged with N_2 for 10 min and loaded into a syringe.

3. Results and Discussions

In our previous studies on photoCMP in flow, we had largely focused on methyl acrylate, MA (and to some extend methyl methacrylate, MMA) as the simplest member of the (meth) acrylate families, in order to provide a proof of concept study. While reactions with MA and MMA were largely successful and convincingly demonstrated the superiority of using flow reactors for photoRDRP, only relatively simple polymers from a materials point of view were in this way generated. Testing which other monomers are suitable for photoflow is, hence, almost obligatory, in order to establish also how far the observed kinetics to date may also hold if the polarity of the ester side chain is changed.

Thus, a broad range of different acrylic monomers was polymerized via photoCMP in a continuous-flow reactor. As representatives for linear hydrophobic monomers, methyl (MA), ethyl (EA), and *n*-butyl acrylate (*n*BA) were chosen. Comparison of this short series of monomers helps to reveal the influence of the ester size on the polymerization performance. As more polar counterparts, 2-hydroxyethyl acrylate (HEA) and di (ethylene glycol) ethyl ether acrylate (DEGA) were tested, to cover also synthetically more interesting materials (see Scheme 1 for structures of all monomers). All polymers were synthesized in a relatively simple but efficient continuous

Scheme 1. Reaction scheme for photo-induced copper-mediated polymerization (photoCMP) and the used acrylate monomers

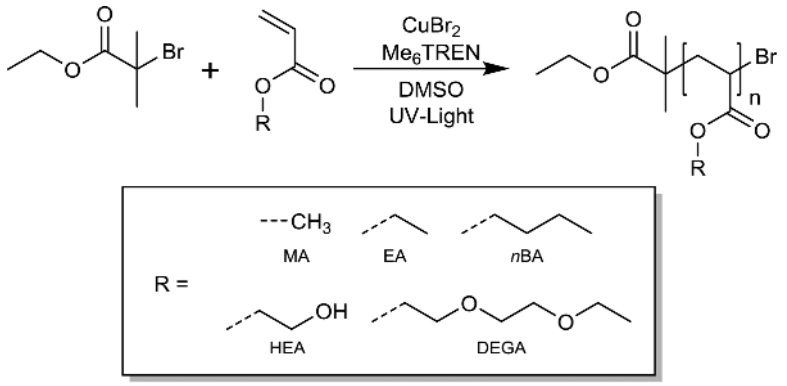

tubular flow reactor consisting of PFA tubing wrapped around a UV-light tube and a syringe pump to deliver the reaction solutions. The reaction is defined by the residence time of the solution in the reactor which is directly correlated to the pump flow rate. In line with our previous study, all polymerizations were performed in DMSO between 50 and 55 °C (it must be noted that the temperature is a consequence of heat-up of the light source during reactor operation) with reaction times up to 20 min. In principle, longer reaction times could be used, but in order to allow for reasonable space-time yields, 20 min was chosen as an aribtrary maximum reaction time. Previous studies show that, within 20 min of monomer conversion, up to 95% are reached and longer reaction times did not lead to significantly higher conversions [16]. Performing the reaction at temperature between 50 and 55 °C is yielding similar polymers as if reactions are carried out at 20 °C [16]. At least within this temperature window, no dependence of the reaction on temperature is observed, hinting at the strong correlation of the initiation mechanism with the overall rate of reaction. As initiator EBiB was used, in a ratio of 1:0.02:0.12 for [EBiB]–[$CuBr_2$]–[Me_6TREN]. All components were dissolved in solvent, degassed, and transferred into a plastic syringe. A second syringe was filled with degassed monomer with ratios of 25 or 45 to initiator and in a volumtric solvent ratio of 1:1. Both solutions were mixed right before entering the reactor in a static T-mixer. Using static mixers to ensure fast and efficient mixing is crucial for high polymerization rates, since slow mixing will result in imperfect initiation at shorter residence times [31]. All polymerizations show high reaction rates with monomer conversions between 76 and 94% within 20-min reaction time (see Table 1 for details). As important as high reaction rates for RDRP are, it is even more crucial to have a good control over the reaction and the length of the obtained polymer. Hence, linear first order kinetic plots with respect to monomer concentartion must be observed (demonstrating a constant radical concetration and, hence, absence of radical termination), alongside linear growth of the polymer material. For all polymers, the measured number average molecular weights are in good agreement with the theoretically calculated values (Table 1). Dispersities are around 1.1, indicating rather narrow molecular weight distributions (MWD) and a high control over the polymerizations. The narrow distributions thereby do not only indicate good control but also underpin that the residence time distribution (RTD) of the polymer is narrow as well, since axial diffusion would increase the RTD and, hence, the overall dispersity of the resulting polymer. Only *n*BA is associated with a slighly increased dispersity of 1.2, which may, however, still be regarded as in line with the other results. A similarly deviating behavior was reported previously for photoCMP polymerization of *n*BA in batch [15a]. Overall, slight differences in reaction rate are observed, and it must be noted that the reaction time of 20 min was chosen arbitrarily. The variation seen between the different monomers indicates that each monomer system must be individually optimized with respect to optimal residence time. The data gathered herein are – as described above – a good indication for the livingness and high level of control over the polymerization, yet, what is regarded an optimum conversion is dependent on the later application and also corresponds to the specific reactor design to a certain degree. However, even after slight adjustment of residence times per monomer (note that, in an attempt to upscale the reaction, 40 min was used for this specific reason; see below), no significantly different results with respect to molecular weight and dispersity must be expected (Table 2).

The kinetic first-order plots for all polymerizations show the required linear behavior (Figure 1), again, underpinning the high level of control over the chain growth that is reached. Only few side reactions seemingly occur, and termination and radical transfer play no significant role in the reaction. Yet, different slopes are observed in the plots, and a significant rate of increase is observed for HEA, which can likely be correlated

Table 2. Target degree of polymerization (at hypothetical full monomer conversion), conversion after 20-min reaction time, and theoretical and experimental number-average molecular weight and dispersity for a series of methyl acrylate polymerizations

	DP	Conversion (%)	$M_{n,theo}$ (g/mol)	$M_{n,GPC}$ (g/mol)	$Đ$
1	45	77	3,100	2,600	1.12
6	100	58	5,100	3,700	1.13
7	150	77	10,000	9,300	1.10
8	200	64	11,000	8,800	1.18
9	300	55	14,300	12,600	1.15
10	400	63	21,800	19,900	1.14
11	500	49	21,200	16,400	1.14

Table 1. Overview over the obtained polymers from photoCMP in a continuous-flow reactor for different acrylate monomers after 20-min reaction time

	Monomer	In–$CuBr_2$–Li–M	Conversion (%)	$M_{n,theo}$ (g/mol)	$M_{n,GPC}$ (g/mol)	$Đ$
1	MA	1:0.02:0.12:45	77	3,100	2,600	1.12
2	EA	1:0.02:0.12:45	76	3,600	2,200	1.11
3	*n*BA	1:0.02:0.12:25	90	3,000	3,200	1.23
4	HEA	1:0.02:0.12:25	94	2,900	1,200	1.07
5	DEGA	1:0.02:0.12:25	83	4,000	3,000	1.10

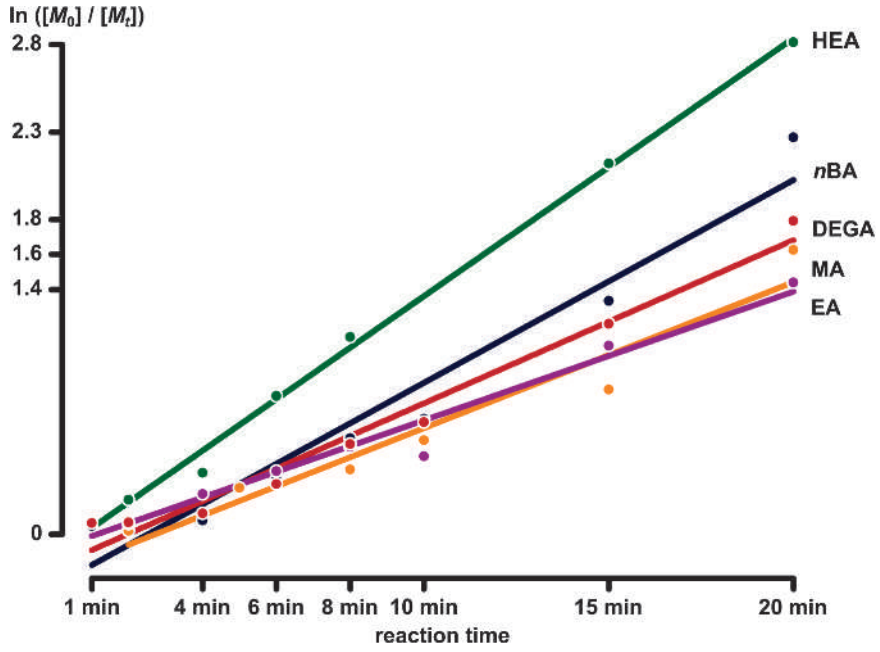

Figure 1. Kinetic first-order plots for the photoCMP polymerization in DMSO of different acrylates in a continuous tubular photoflow reactor

to a faster propagation of this monomer in highly polar media compared to the other monomers. Extrapolation of the plots allows to determine what reaction times are, in principle, required to reach higher conversions.

3.1. Increasing Chain Length. After showing the wide applicability of photoCMP with different acrylate monomers, the limits of the reaction concerning polymer chain length were tested. Increasing chain length is associated with different problems. Higher molecular weight material causes higher viscosities, and, hence, leads to increased pressure drops and eventually clogging of the reactor system. At the same time, characteristic for photoCMP, a lower polymerization rate must be expected when the initiator concentration is lowered (less bromine available for chain initiation). To our best knowledge, until today, only degrees of polymerization (DP) up to 100 have been reported in literature for photoCMP flow processes. In here, the DP is increased step wise, which corresponds to molecular weights in the range of 20 000 g/mol. All polymerizations were done with a 1:3 dilution in DMSO (25 vol% monomer to 75 vol% DMSO). Target degrees of polymerizations were set to 500; however, due to limitations in the reaction rate (see above), maximum DP reached in practice were about 250. Reaching higher chain lengths is difficult and often leads to a loss of control over the polymerization, which can probably be linked to the then lower bromine concentration, which is required in the photoinitiation process. This limitation is, however, not specific to the flow process and applies also to batch photoCMP reactions. Nevertheless, for most applications of high-precision polymer materials (i.e., biomedical use) as described herein, polymer chains are no longer required. The polymerizations were again performed in a continuous tubular reactor equipped with a 15-Watt UV-light tube. For increasing targeted DP, an increase in number average molecular weight was observed, even if monomer conversions reached within 20 min decreased in accordance to the lowered initiation rate. In Figure 2, the MWD of polymers obtained after polymerizations of 20 min are given, depicting a clear shift to higher molecular weights with increasing targeted DP. Interestingly, while a rate reduction is observed, no quality loss in the product is seen, and all polymers are constant within error limits with respect to dispersity. All molecular weights obtained are all in good agreement to calculated theoretical values, when monomer conversion is taken into account.

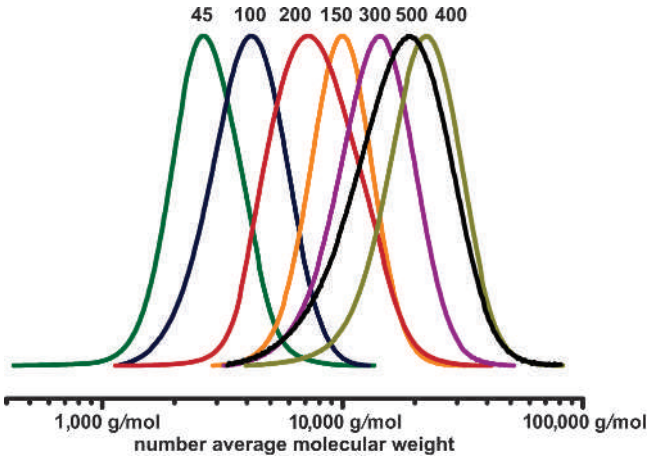

Figure 2. Molecular weight distributions for polymers made in continuous-flow photoCMP of methyl acrylate under variation of the initiator concentration in order to produce materials with different target molecular weight

3.2. PhotoCMP in H_2O–EtOH as Solvent. PhotoCMP is routinely carried out in DMSO. Yet, other polar solvents are equally suitable, with alcohol–water mixtures being a benign alternative. It should be noted that, ideally, polymerizations are most interesting when being carried out in pure water; however, to date, for batch reactions, this has also been shown to lead to a loss of control for the photoCMP reaction. This is somewhat in contrast to classical SET-LRP polymerizations, where pure water is a common solvent [32]. In here, we tested if the photoCMP reaction is suitable for flow processing when being carried out in a 50:50 vol% H_2O–ethanol solvent mixture, since such conditions had also for batch been shown to be successful. For these tests, the water soluble monomer DEGA was used. The initiator was changed from EBiB to the more hydrophilic HMB (Scheme 2). For the polymerization, different chain lengths are targeted to show again the robustness of the system. Reactions with target DP of 25, 50, and 100 were carried out, reaching almost quantitative conversion of monomer in all

Scheme 2. Reaction scheme for the synthesis of pDEGA in H2O/EtOH (50:50 vol%) via photoCMP

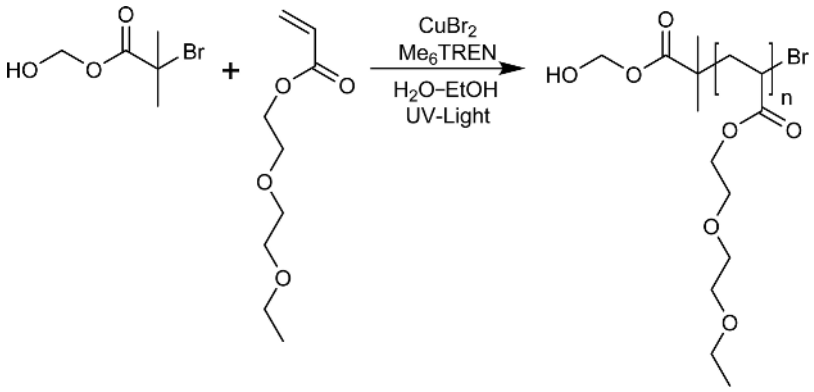

Table 3. Number-average molecular weights, dispersities, and conversion for the polymerization of DEGA via photoCMP in 50:50 vol% H_2O–EtOH in a photoflow reactor

	DP	Conversion (%)	$M_{n,theo}$ (g/mol)	$M_{n,GPC}$ (g/mol)	$Đ$
12	25	98	4,800	5,600	1.22
13	50	98	9,400	6,900	1.23
14	100	92	17,500	12,800	1.17

cases within 20-min reaction time (Table 3). In comparison to the polymerization of DEGA in DMSO (see Table 1, line 5), the conversion increased by 15%, which may again be attributed to polar effects on the propagation rate of the monomer. However, the reaction in DMSO provided material with slightly better dispersity compared to reaction carried out in H_2O–EtOH.

Number-average molecular weights up to 13,000 g/mol within 20-min reaction time were reached (Figure 3). Closer inspection of the kinetics reveals that 20 min in these cases is almost not necessary as conversions above 90% are observed already after 10 min, which, in many cases, might be regarded as sufficient for synthesis purposes. On the other hand, extending the reactor residence time also has no destructive influence on the reaction outcome. Dispersities remain widely constant, indicating that the polymerization comes to a mere halt rather than entering side reactions when monomer concentration diminishes (as is often observed for other RDRP techniques).

3.3. Upscaling of PhotoCMP in Continuous Flow. As described, the main advantage of using continuous flow for photopolymerizations is the scalability of the reaction. When carried out in batch, photoCMP is usually carried out in lower gram scale or less due to rapid efficiency losses when larger optical path lengths are required. Thus, the ability to go beyond this limitation was tested for the above described flow reactor

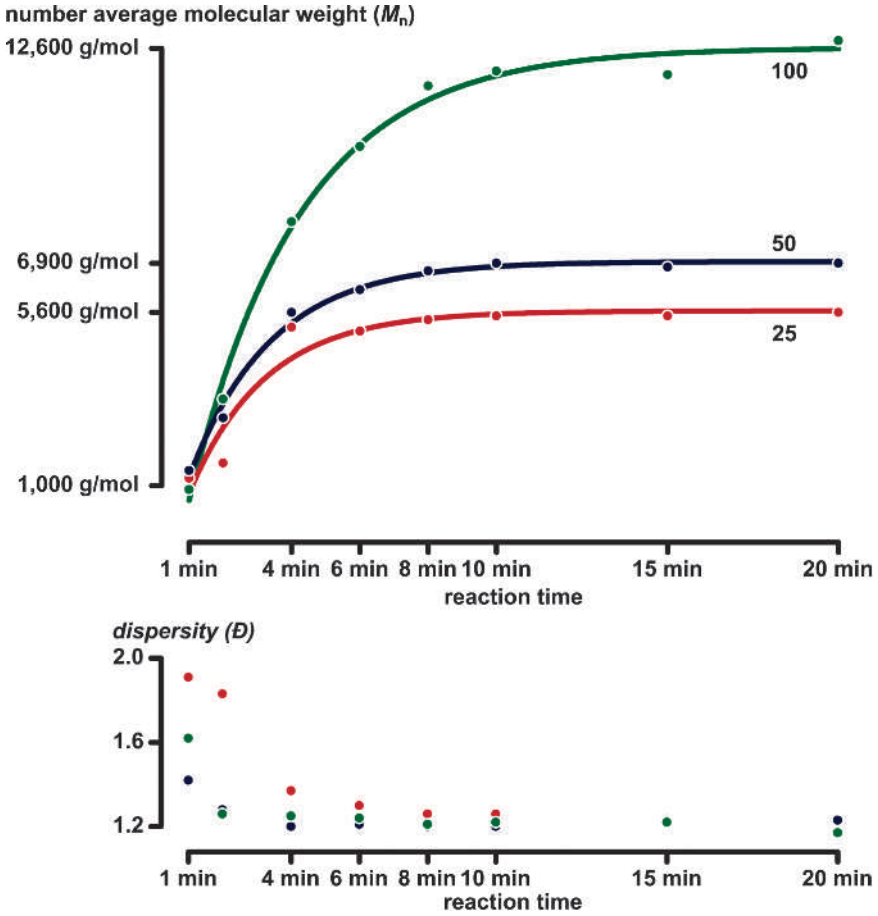

Figure 3. Evolution of number average molecular weights and dispersities of pDEGA in photoCMP using a 50/50 vol% H_2O–EtOH mixture as solvent for various target DP

design. Whereas the above polymerizations were carried out in a 2-mL reactor with 0.75 mm inner diameter, the first scale-up was performed by employing PFA tubing with an inner diameter of 1 mm (outer diameter 1/16″) and a total internal volume of 16 mL was used (see right side of Figure 4). Such reactor is still relatively small and can easily be operated in a standard fume cupboard. Two Knauer Azura P2.1S HPLC pumps were used to deliver the two reaction solutions, which were otherwise chosen accordingly to the previous experiments (first solution containing initiator [EBiB, 1 eq.], $CuBr_2$ [0.02 eq.], Me_6TREN [0.12 eq.], and DMSO; second feed was bulk methyl acrylate). Also, in this case, a relatively simple static T-mixer was used to combine both feed streams. Comparison of the MA results from this study and the work of Wenn et al. shows identical yields even when using different UV light sources and pumps [16]. Wenn et al. had also shown that an upscale from a microflow system (reactor volume = 19.5 μL, width channel = 300 μm, depth channel = 120 μm) to milliflow devices does not require tedious reoptimization and that conditions identified for microflow devices are directly translatable to larger flow reactors. This underlines the robustness of this reaction in continuous photoflow processing. Hence, switching from syringe to HPLC pumps has no significant influence on the reaction or the yield. At a reaction time of 40 min, this reactor setup produces roughly 11 g of pMA per hour with a number average molecular weight of 3,000 g/mol and a dispersity of 1.1. Important to note is that, if the reaction conditions would change during operation of the reactor (due to fouling, inconsistent mass transport due to the viscous flow), then, inevitably, a broadening of the molecular weight distribution of the collected material should occur, as variations in residence time will lead to variations in absolute molecular weight as well. A reaction time of 40 min was chosen for the upscaling experiments to reach a monomer conversion above 90%. This residence time was picked conservatively to demonstrate the broad validity of the approach. With 20-min reaction time, only slightly smaller polymers would have been obtained. The reactor was operated continuously for 18 h, yielding over 200 g of high quality polymer (see Figure 4) and still retaining very narrow molecular weight distributions. No further reaction optimization was required to achieve this upscale from the 2 mL to the 16 mL reactor. Further, 200 g of material

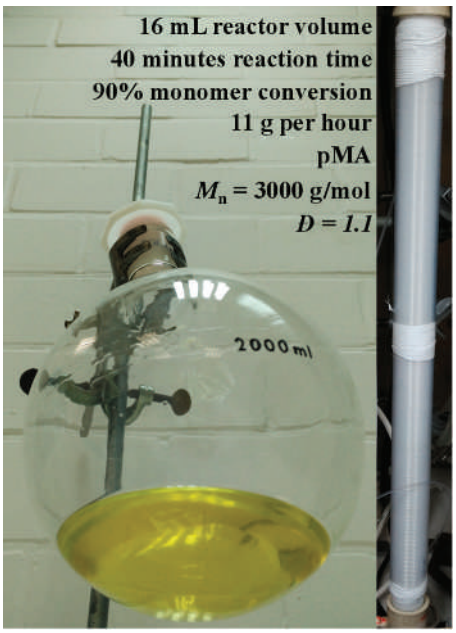

Figure 4. Photo of the tubular flow reactor with an internal volume of 16 mL (right) and the 200 g pMA obtained by collection of product over 18 h in the same reactor (left)

for high precision photoCMP polymers may be regarded as a very significant production scale (due to the very high value of these materials). Even in conventional thermal batch polymerizations, such quantities are not easily reached on laboratory scale and usually require dedicated equipment and stringent optimization routines. Possible applications of such high precision polymers range from the biomedical field and nanomedicine to high-performance dispersants in ink formulation. In these realms, often, only kilograms are required in production rather than ton scales.

Thus, scale-up of the reaction is indeed simple, and reactor setups that produce 100 or more grams of highly precise polymers per hour should be no significant hurdle, and even larger amounts may only be limited by the available light choice. In fact, literature studies have demonstrated the possibility of easy upscale for continuous photoflow reactions [33]. It should be noted that, throughout this study, no performance decrease was observed with the used reactor. In principle, long-time exposure of the tubing to UV light can lead to material ageing and, at a certain point, lead to failure of the equipment. Since the employed UV light sources are rather low intensity, it is however, expected that such failure would only occur after longer time periods and that material failure is prevented in the regular maintenance cycles of such devices. Reactor tubing is comparatively cheap and is replacement on a frequent basis in a production facility would not pose a significant hurdle.

3.4. Reactor Cascade for One-Step Chain Extension. The full potential of RDRP reactions unfolds when more complex materials are targeted, by making use of sequential polymerization approaches. By isolation of polymer, followed by mixing with fresh monomer and catalyst, block copolymers become available after reinitiation. Especially when polymers with different solubility and miscibility are used, interesting materials in this way can be quickly synthesized. We had shown before that photoCMP-made block copolymers are available from flow processes, when polymers are isolated after the first reactor stage. The purification between the two reactions makes the process labor intensive and, thus, expensive. Using a reactor cascade can solve this problem, as in case almost all monomer is used up in the first reaction stage, no purification is in fact required before addition of fresh monomers. Two serial flow reactors, hence, give direct access to (multi) block copolymers [34].

Consequently, the reactor setup was extended by a second stage. In principle, no additional light source is required as the tubing for both stages can conveniently be wrapped around the same UV-light tube. Two reaction solutions were prepared, degassed, and filled in individual plastic syringes. One reaction solution contained the initiator, $CuBr_2$, Me_6TREN, and the solvent. The second syringe was used to deliver the first monomer batch (DEGA). Both solutions were mixed in a static T-mixer before entering the reactor tube which was wrapped around the UV-light tube. The exit of this reactor was connected with a second static T-mixer where the second monomer H_2O–EtOH solution was added. Dilution is required in the second stage to avoid increasing viscosities with increasing polymer chain length. Polymer samples are collected after the first reactor stage and after passing through both stages. The experimental setup is schematically given in Figure 5. It should be noted that, in the present case, DEGA was used for both polymer blocks; hence, no true block copolymer was obtained. Yet, DEGA is a very interesting monomer for amphiphilic block copolymer synthesis, and it is more convenient to chain extend with the same monomer for the sake of simpler polymer analysis (no change in Mark-Houwink parameters), an approach that is often taken in fundamental investigations into chain extension reactions. In principle, the second monomer could

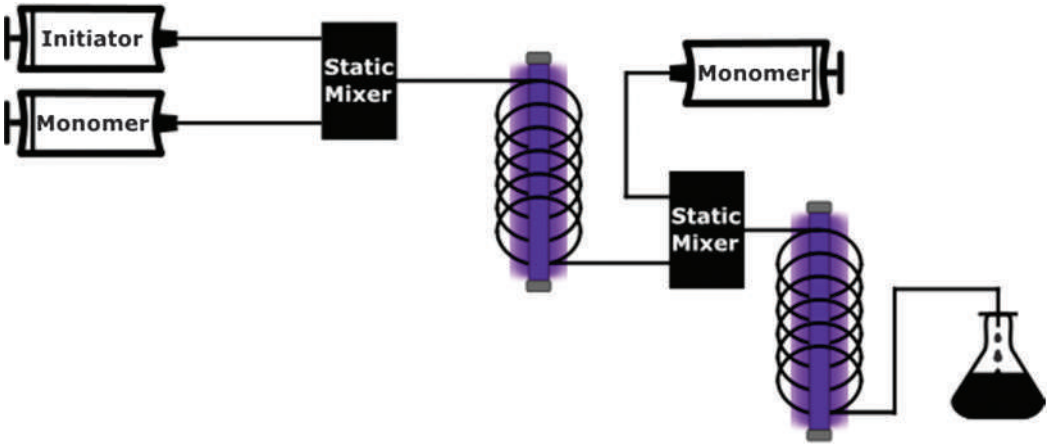

Figure 5. Schematic photoflow reactor setup for the one-step synthesis of diblock copolymers

be replaced by any alkyl acrylate; only exact molecular weight determination would be slightly influenced by the choice of monomer.

Two examples of successful one-step chain extension reactions in batch reactors via photoCMP are reported [35]. In both approaches, DMSO was employed. In here, we adopted the above-tested H_2O–EtOH system to demonstrate the working principle of the coupled reactor setup, not only to accelerate block copolymer synthesis but also provide greener processing conditions at the same time. The reactor residence times were in both reactor stages set to 10 min, which allowed for a monomer conversion of 83% and a number average molecular weight of 4,500 g/mol ($Đ$ = 1.19, theoretical molecular weight of 4,100 g/mol; see Figure 6) in the first stage. The reactor outlet was then directly mixed with a DEGA–H_2O–EtOH solution (50:25:25 vol%) and injected in the second reactor. After further 10-min reaction time, a polymer with a total molecular weight of 6,500 g/mol (theoretical molecular weight of 6,100 g/mol) and a dispersity of 1.2 was collected (Figure 6). In principle, the described reactor is able to produce true block copolymers also, yet, in order to avoid gradient blocks, it is important to bring the reaction to almost complete monomer conversion (>97%) or to remove the unreacted monomer before the second monomer is added. Nevertheless, no significant reactivity differences between various acrylate monomers must be expected and results will be directly extrapolatable to any other member of the monomer family.

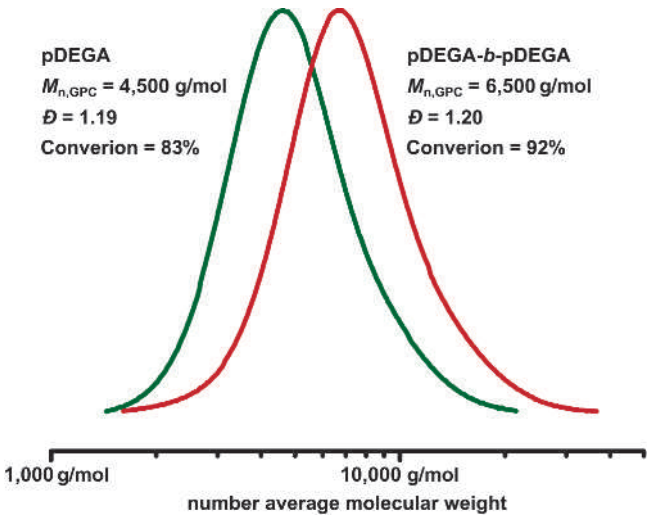

Figure 6. Molecular weight distributions of polymer obtained after the first and after the second reactor stage (both residence times set to 10 min per reactor coil)

4. Conclusions

The synthetic scope of photo-induced copper-mediated polymerization in continuous-flow reactors has been expanded. A large variety of acrylate monomers was successfully polymerized in tubular reactors in reaction times up to 20 min with monomer conversions between 77 and 94%. The quality of the polymer products is throughout the series of monomers high, as indicated by the good agreement between calculated and experimentally obtained molecular weight and low dispersity (<1.2) of the products. Further, the regularly used solvent DMSO can be exchanged for an ethanol–water mixture when polar monomers are used, making the process inherently greener. The first scale-up of the polymerizations is successful, hinting also at the commercial viability of the photopolymerization, with over 200 g of high-definition polymer materials being available without large efforts in a relatively small sized photoreactor (16 mL internal volume). As the last step, the coupling of two continuous photoflow reactors for direct chain extension reactions has been demonstrated for the first time.

Acknowledgments. The authors are grateful for support by the Belgian Science Policy (BELSPO) via the Interuniversity Attraction Poles Program IAP P7/05 “Functional Supramolecular Systems.” T.J. wishes to thank the Fonds Wetenschappelijk Onderzoek (FWO) for a research grant. Further, assistance in laboratory work during the internships of Axel-Laurenz Buckinx and Dries Wyers is kindly acknowledged.

References

1. Oelgemöller, M.; Shvydkiv, O. *Molecules* **2011**, *16*, 7522–7550.
2. Junkers, T.; Wenn, B. *React. Chem. Eng.* **2016**, *1*, 60–64.
3. Hook, B. D. A.; Dohle, W.; Hirst, P. R.; Pickworth, M.; Berry, M. B.; Booker-Milburn, K. I. *J. Org. Chem.* **2005**, *70*, 7558–7564.
4. Su, Y.; Kuijpers, K.; Hessel, V.; Noel, T. *React. Chem. Eng.* **2016**, *1*, 73–81.
5. Derboven, P.; Van Steenberge, P. H. M.; Vandenbergh, J.; Reyniers, M.-F.; Junkers, T.; D'Hooge, D. R.; Marin, G. B. *Macromol. Rapid Commun.* **2015**.
6. Chiefari, J.; Chong, Y. K.; Ercole, F.; Krstina, J.; Jeffery, J.; Le, T. P. T.; Mayadunne, R. T. A.; Meijs, G. F.; Moad, C. L.; Moad, G.; Rizzardo, E.; Thang, S. H. *Macromolecules* **1998**, *31*, 5559–5562.
7. Nicolas, J.; Guillaneuf, Y.; Lefay, C.; Bertin, D.; Gigmes, D.; Charleux, B. *Prog. Polym. Sci.* **2013**, *38*, 63–235.
8. Boyer, C.; Corrigan, N. A.; Jung, K.; Nguyen, D.; Nguyen, T.-K.; Adnan, N. N. M.; Oliver, S.; Shanmugam, S.; Yeow, J. *Chem. Rev.* **2016**, *116*, 1803–1949.
9. Coessens, V.; Pintauer, T.; Matyjaszewski, K. *Prog. Polym. Sci.* **2001**, *26*, 337–377.
10. Haddleton, D. M.; Crossman, M. C.; Hunt, K. H.; Topping, C.; Waterson, C.; Suddaby, K. G. *Macromolecules* **1997**, *30*, 3992–3998.
11. (a) Guillaneuf, Y.; Bertin, D.; Gigmes, D.; Versace, D.-L.; Lalevée, J.; Fouassier, J.-P. *Macromolecules* **2010**, *43*, 2204–2212; (b) Quinn, J. F.; Barner, L.; Barner-Kowollik, C.; Rizzardo, E.; Davis, T. P. *Macromolecules* **2002**, *35*, 7620–7627; (c) Tasdelen, M. A.; Uygun, M.; Yagci, Y. *Macromol. Rapid Commun.* **2011**, *32*, 58–62.
12. Detrembleur, C.; Versace, D.-L.; Piette, Y.; Hurtgen, M.; Jerome, C.; Lalevee, J.; Debuigne, A. *Polym. Chem.* **2012**, *3*, 1856–1866.

13. Liang, E.-X.; Zhong, M.; Hou, Z.-H.; Huang, Y.; He, B.-H.; Wang, G.-X.; Liu, L.-C.; Wu, H. *J. Macromol. Sci., Part A* **2016**, *53*, 210–214.
14. Treat, N. J.; Fors, B. P.; Kramer, J. W.; Christianson, M.; Chiu, C.-Y.; Alaniz, J. R. d.; Hawker, C. J. *ACS Macro Lett.* **2014**, *3*, 580–584.
15. (a) Anastasaki, A.; Nikolaou, V.; Zhang, Q.; Burns, J.; Samanta, S. R.; Waldron, C.; Haddleton, A. J.; McHale, R.; Fox, D.; Percec, V.; Wilson, P.; Haddleton, D. M. *J. Am. Chem. Soc.* **2014**, *136*, 1141–1149; (b) Konkolewicz, D.; Schröder, K.; Buback, J.; Bernhard, S.; Matyjaszewski, K. *ACS Macro Lett.* **2012**, *1*, 1219–1223; (c) Tasdelen, M. A.; Uygun, M.; Yagci, Y. *Macromol. Chem. Phys.* **2011**, *212*, 2036–2042.
16. Wenn, B.; Conradi, M.; Carreiras, A. D.; Haddleton, D. M.; Junkers, T. *Polym. Chem.* **2014**, *5*, 3053–3060.
17. Chuang, Y.-M.; Wenn, B.; Gielen, S.; Ethirajan, A.; Junkers, T. *Polym. Chem.* **2015**, *6*, 6488–6497.
18. Wenn, B.; Martens, A. C.; Chuang, Y.-M.; Gruber, J.; Junkers, T. *Polym. Chem.* **2016**, *7*, 2720–2727.
19. Kermagoret, A.; Wenn, B.; Debuigne, A.; Jerome, C.; Junkers, T.; Detrembleur, C. *Polym. Chem.* **2015**, *6*, 3847–3857.
20. Melker, A.; Fors, B. P.; Hawker, C. J.; Poelma, J. E. *J. Polym. Sci., Part A: Polym. Chem.* **2015**, *53*, 2693–2698.
21. Laun, J.; Vorobii, M.; de los Santos Pereira, A.; Pop-Georgievski, O.; Trouillet, V.; Welle, A.; Barner-Kowollik, C.; Rodriguez-Emmenegger, C.; Junkers, T. *Macromol. Rapid Commun.* **2015**, *36*, 1681–1686.
22. Vandenbergh, J.; Reekmans, G.; Adriaensens, P.; Junkers, T. *Chem. Sci.* **2015**, *6*, 5753–5761.
23. (a) Chen, M.; Johnson, J. A. *Chem. Commun.* **2015**, *51*, 6742–6745; (b) Gardiner, J.; Hornung, C. H.; Tsanaktsidis, J.; Guthrie, D. *Eur. Polym. J.* **2016**, *80*, 200–207.
24. Baeten, E.; Vanslambrouck, S.; Jérôme, C.; Lecomte, P.; Junkers, T. *Eur. Polym. J.* **2016**, *80*, 208–218.
25. Pan, X.; Tasdelen, M. A.; Laun, J.; Junkers, T.; Yagci, Y.; Matyjaszewski, K. *Prog. Polym. Sci.* **2016**, doi:10.1016/j.progpolymsci.2016.06.005.
26. Feng, L.; Hu, J. W.; Liu, Z. L.; Zhao, F. B.; Liu, G. J. *Polymer* **2007**, *48*, 3616–3623.
27. Yin, Z.; Koulic, C.; Pagnoulle, C.; Jérôme, R. *Macromolecules* **2001**, *34*, 5132–5139.
28. Barner-Kowollik, C.; Beuermann, S.; Buback, M.; Castignolles, P.; Charleux, B.; Coote, M. L.; Hutchinson, R. A.; Junkers, T.; Lacík, I.; Russell, G. T.; Stach, M.; van Herk, A. M. *Polym. Chem.* **2014**, *5*, 204–212.
29. Asua, J. M.; Beuermann, S.; Buback, M.; Castignolles, P.; Charleux, B.; Gilbert, R. G.; Hutchinson, R. A.; Leiza, J. R.; Nikitin, A. N.; Vairon, J.-P.; van Herk, A. M. *Macromol. Chem. Phys.* **2004**, *205*, 2151–2160.
30. Appelt, B.; Meyerhoff, G. *Macromolecules* **1980**, *13*, 657–662.
31. (a) Bally, F.; Serra, C. A.; Hessel, V.; Hadziioannou, G. *Chem. Eng. Sci.* **2011**, *66*, 1449–1462; (b) Hessel, V. *Chem. Eng. Technol.* **2009**, *32*, 1655–1681.
32. (a) Tsarevsky, N. V.; Pintauer, T.; Matyjaszewski, K. *Macromolecules* **2004**, *37*, 9768–9778; (b) Bortolamei, N.; Isse, A. A.; Magenau, A. J. D.; Gennaro, A.; Matyjaszewski, K. *Angew. Chem. Int. Ed.* **2011**, *50*, 11391–11394; (c) Konkolewicz, D.; Krys, P.; Góis, J. R.; Mendonça, P. V.; Zhong, M.; Wang, Y.; Gennaro, A.; Isse, A. A.; Fantin, M.; Matyjaszewski, K. *Macromolecules* **2014**, *47*, 560–570.
33. Knowles, J. P.; Elliott, L. D.; Booker-Milburn, K. I. *Beilstein J. Org. Chem.* **2012**, *8*, 2025–2052.
34. (a) Baeten, E.; Verbraeken, B.; Hoogenboom, R.; Junkers, T. *Chem. Commun.* **2015**, *51*, 11701–11704; (b) Hornung, C. H.; Nguyen, X.; Kyi, S.; Chiefari, J.; Saubern, S. *Aust. J. Chem.* **2013**, *66*, 192–198; (c) Nagaki, A.; Takahashi, Y.; Akahori, K.; Yoshida, J.-i. *Macromol. React. Eng.* **2012**, *6*, 467–472.
35. (a) Chuang, Y.-M.; Ethirajan, A.; Junkers, T. *ACS Macro Letters* **2014**, *3*, 732–737; (b) Anastasaki, A.; Nikolaou, V.; McCaul, N. W.; Simula, A.; Godfrey, J.; Waldron, C.; Wilson, P.; Kempe, K.; Haddleton, D. M. *Macromolecules* **2015**, *48*, 1404–1411.